Atmos. Chem. Phys., 24, 11351–11363, 2024
https://doi.org/10.5194/acp-24-11351-2024


Atmospheric Chemistry and Physics
Open Access
EGU



# Measurement report: Urban ammonia and amines in Houston, Texas

**Lee Tiszenkel[1], James H. Flynn[2], and Shan-Hu Lee[1]**

[1]Department of Atmospheric and Earth Sciences, University of Alabama at Huntsville, Huntsville, Alabama, USA
[2]Department of Earth and Atmospheric Sciences, University of Houston, Houston, Texas, USA

**Correspondence:** Shan-Hu Lee (shanhu.lee@uah.edu)

Received: 26 April 2024 – Discussion started: 7 May 2024
Revised: 23 August 2024 – Accepted: 1 September 2024 – Published: 11 October 2024

**Abstract.** Ammonia and amines play critical roles in secondary aerosol formation, especially in urban environments. However, fast measurements of ammonia and amines in the atmosphere are very scarce. We measured ammonia and amines with a chemical ionization mass spectrometer (CIMS) at the urban center in Houston, Texas, the fourth most populated urban site in the United States, during October 2022. Ammonia concentrations were on average four parts per billion by volume (ppbv), while the concentration of an individual amine ranged from several parts per trillion by volume (pptv) to hundreds of pptv. These reduced nitrogen compounds were more abundant during weekdays than on weekends and correlated with measured CO concentrations, implying they were mostly emitted from pollutant sources. Both ammonia and amines showed a distinct diurnal cycle, with higher concentrations in the warmer afternoon, indicating dominant gas-to-particle conversion processes taking place with the changing ambient temperatures. Studies have shown that dimethylamine is critical for new particle formation (NPF) in the polluted boundary layer, but currently there are no amine emission inventories in global climate models (as opposed to ammonia). Our observations made in the very polluted area of Houston, as well as a less polluted site (Kent, Ohio) from our previous study (You et al., 2014), indicate there is a consistent ratio of dimethylamine over ammonia at these two sites. Thus, our observations can provide a relatively constrained proxy of dimethylamine using 0.1 % ammonia concentrations at polluted sites in the United States to model NPF processes.

## 1 Introduction

Atmospheric ammonia and amines are ubiquitous in the atmosphere, and they have been found in the gas phase and in aerosols, clouds, and fog droplets (Ge et al., 2011a, b). Ammonia and amines are emitted from various natural and anthropogenic sources, such as agricultural activity, animal husbandry, vegetation, soil, waste processing, automobile traffic, power plants, and biomass burning (Ge et al., 2011a). Ammonia and amines often share the same emission sources. In general, ambient concentrations of ammonia are at the parts per billion by volume (ppbv) range, and amines are approximately 2 to 3 orders of magnitude lower than ammonia concentrations. Ambient concentrations of ammonia and amines vary rapidly due to emission, gas-to-particle conversion, and wet-deposition processes (You et al., 2014; Yu and Lee, 2012 ).

Laboratory studies have shown that ammonia and amines play key roles in new particle formation (NPF) as they can stabilize sulfuric acid clusters (Yu et al., 2012; Almeida et al., 2013; Lehtipalo et al., 2018; Xiao et al., 2021; Glasoe et al., 2015; Jen et al., 2016). In particular, dimethylamine can have a profound effect on atmospheric processes even at the parts per trillion by volume (pptv) level (Almeida et al., 2013; Glasoe et al., 2015). Field observations show that ammonia and amines are associated with NPF events in Chinese megacities (Yao et al., 2016; Yan et al., 2021; Cai et al., 2021, 2023), urban areas in the United States (Jen et al., 2016; Smith et al., 2010), European cities (Brean et al., 2020), a

high-altitude site (Bianchi et al., 2016), and the Arctic and Antarctic (Beck et al., 2021; Brean et al., 2021; Jokinen et al., 2018; Köllner et al., 2017). However, global models cannot simulate urban NPF processes currently because of the lack of amine emission inventories in models.

Ammonia and amines also contribute to secondary organic aerosol (SOA) formation by condensation of oxidation products formed by reactions with ozone, OH, or $NO_3$ radicals and produce light-absorbing particles (Erupe et al., 2010; Malloy et al., 2009; Silva et al., 2008; Nielsen, 2016; Nielsen et al., 2012; Qiu and Zhang, 2013). As a result, reducing ammonia emissions has been identified as a cost-effective way to mitigate ambient fine-particle concentrations (Gu et al., 2021).

Fast-response measurements of ammonia and amines at atmospheric concentrations are very challenging (Lee, 2022), although such measurements are necessary because these reduced nitrogen compounds have relatively short atmospheric lifetimes (Nielsen et al., 2012). Previously, Schwab et al. (2007) made an intercomparison of six different ammonia detection methods in the laboratory and found a large variance in the measured concentrations and vastly different response times (over several hours) within different instruments. Difficulties in the detection of base compounds also arise because these "sticky" compounds can rapidly adsorb and desorb on or from the surfaces of sampling inlets to cause background signals that vary depending on ambient concentrations, air humidity, and other atmospheric conditions. Thus, frequent in situ measurements of instrument background signals using proper zero gases are required, especially for field observations with rapidly changing ambient concentrations of base compounds.

Chemical ionization mass spectrometers (CIMS) using ion reagents such as protonated ethanol, acetone, and water ions can detect ammonia and amines in the atmosphere with fast response (Nowak et al., 2006; Benson et al., 2010; Yu and Lee, 2012; Hanson et al., 2011; Jen et al., 2016; Nowak et al., 2010). As summarized in Table 1, the CIMS technique has been used for the detection of ambient ammonia and amines at a polluted site in Ohio (You et al., 2014; Yu and Lee, 2012), a rural Alabama forest (You et al., 2014), and polluted urban sites in China (Zheng et al., 2015; M. Wang et al., 2020; G. Wang et al., 2016; Zhu et al., 2022). As shown in Table 1, there are even fewer studies that simultaneously measured ammonia and amines. The CIMS using ethanol reagents can measure amines at or below single-digit pptv concentrations with a time response of 1 min and simultaneously measure amines and ammonia (You et al., 2014; Yu and Lee, 2012; Erupe et al., 2011; Benson et al., 2010). The CIMS using protonated water ions (i.e., a proton transfer chemical ionization mass spectrometer, PTR-CIMS) can measure monoamines and diamines (Hanson et al., 2011; Jen et al., 2016). Using a high-resolution time-of-flight (HR-TOF) detector coupled to CIMS (HR-TOF CIMS) (with an ethanol reagent), Yao et al. (2016) measured various amines and amides in Shanghai. However, isomers of amines were still not resolved in the detection; for example, the measured $C_2$ amines still contained dimethylamine and ethylamine. Thus, a major disadvantage of a mass spectrometer (regardless of mass resolution) is the inability to resolve and identify isomers. To resolve isomers, tandem MS/MS analysis or an additional independent separation method (such as chromatography) coupled to the mass spectrometer is necessary.

In situ measurements of ammonia have also been made in various atmospheric environments with optical techniques such as open-path absorption (Miller et al., 2014), closed-path absorption (Griffith and Galle, 2000; Ellis et al., 2010; McManus et al., 2010; Leen et al., 2013; Pollack et al., 2019), cavity ring-down spectroscopy (Martin et al., 2016), and photoacoustic spectroscopy (Pushkarsky et al., 2002). These fast-response optical techniques were used for flux and aircraft measurements of ammonia.

We measured ammonia and $C_1$–$C_6$ amines with an ethanol CIMS in October 2022 at the urban center in Houston, Texas. Houston is the fourth most populated urban center in the US and contains a diverse range of pollutant emissions from urban activity, traffic, ship channels, oil production, marine air masses, and agricultural activity. The primary goal of these measurements is to quantify ammonia and $C_1$–$C_6$ amines in an urban setting and identify the atmospheric conditions that affect their abundance. The study is amongst very few observations of ammonia and amines at highly polluted urban sites in the US. We also compare observations in Houston with previous measurements taken with the same instrument in Kent, Ohio (less polluted) (You et al., 2014), and establish a quantitative relationship between ammonia and dimethylamine in a different range of polluted conditions. This relationship will allow global models to simulate urban NPF processes using the existing ammonia emission inventories.

## 2 Methods

The field observation took place in Houston continuously from 8 to 27 October 2022. Measurements were made at a stationary platform located on the campus of the University of Houston (29.72° N, 95.34° W), ∼ 2.5 km from central downtown Houston. Maps of the measurement site (Figs. 1 and S1). The measurement platform was located ∼ 5 m from an active parking lot, ∼ 200 m from a low-traffic road, ∼ 300 m from a high-traffic thoroughfare, and ∼ 500 m from an interstate highway. The immediate vicinity of the site was the University of Houston campus, containing classroom buildings, dormitories, facility services, and dining halls. Nearby (to the southeast of the site) were several restaurants and an industrial park containing sites of chemical supply companies, construction, machining services, and automobile shops. The site was surrounded by residential areas to the south, northeast, and west. The city center and highest

**Table 1.** Ammonia and amine measurements with CIMS at various locations reported in the literature. DL is the detection limit of each instrument.

| Location | $NH_3$ (ppbv) | $C_1$ amine (pptv) | $C_2$ amine (pptv) | $C_3$ amine (pptv) | $C_4$ amine (pptv) | $C_5$ amine (pptv) | $C_6$ amine (pptv) |
|---|---|---|---|---|---|---|---|
| Rural Alabama forest (You et al., 2014)[a] | Up to 1–2 | < DL | < DL | 1–10 | < DL | < DL | < DL |
| Kent, Ohio (You et al., 2014)[a] | Up to 6 | 1–4 | < DL | 5–10 | 10–50 | 10–100 | < DL |
| Kent, Ohio (Yu and Lee, 2012)[a] | $0.5 \pm 0.26$ | – | $8 \pm 3$ | $16 \pm 7$ | – | – | – |
| Atlanta, Georgia (Hanson et al., 2011)[b] | – | < 1 | 3 | 4–15 | 25 | – | – |
| Lewes, Delaware (Freshour et al., 2014)[b] | 0.8 | 5 | 28 | 6 | 150 | 1 | 2 |
| Lamont, Oklahoma (Freshour et al., 2014)[b] | 0.9 | 4 | 14 | 35 | 150 | 98 | 20 |
| Minneapolis, Minnesota (Freshour et al., 2014)[b] | 1.8 | 4 | 42 | 19 | 14 | 20 | 5 |
| Shanghai (Yao et al., 2016)[c] | – | $3.9 \pm 1.2$ | $6.6 \pm 1.2$ | $0.4 \pm 0.1$ | $3.6 \pm 1.0$ | $0.7 \pm 0.3$ | $1.8 \pm 0.8$ |
| Nanjing (Zheng et al., 2015)[c] | $1.7 \pm 2.3$ | $7.2 \pm 7.4$ ($C_1 + C_2 + C_3$) | | | – | – | – |
| Wangdu (Y. Wang et al., 2020)[d] | – | – | $14.6 \pm 14.9$ | – | – | – | – |
| Beijing (Zhu et al., 2022)[c] | $2.8 \pm 2.0$ | $5.2 \pm 4.3$ ($C_1 + C_2 + C_3$) | – | – | – | | |
| Houston, Texas (This study)[a] | $4 \pm 1$ | $4 \pm 2$ | $6 \pm 2$ | $31 \pm 9$ | $79 \pm 30$ | $33 \pm 12$ | $12 \pm 4$ |

[a] CIMS with an ethanol reagent. [b] Proton transfer chemical ionization mass spectrometer (PTR-CIMS). [c] High-resolution time-of-flight chemical ionization mass spectrometer (HR-TOF CIMS) with ethanol reagent. [d] Vocus proton transfer time-of-flight mass spectrometer (PTR-TOF MS).

population densities were to the northeast of the measurement site.

The ethanol CIMS instrument used has been described in detail previously (Benson et al., 2010; You et al., 2014; Yu and Lee, 2012). The CIMS draws 10 standard liter per minute (slpm) of sample air into a low-pressure ion–molecule region (about 2000 Pa) where the flow mixes with a pure nitrogen flow at 2 slpm through a stainless-steel vessel of 200 proof ethanol, followed by a $^{210}P_o$ radiation source. Ammonia and amines were detected with the following ion molecule reactions based on Erupe et al. (2011), Yu and Lee (2012), and Nowak et al. (2006):

$$(C_2H_5OH)_nH^+ + NH_3 \rightarrow (C_2H_5OH)_{n-1}NH_4^+ + C_2H_5OH, \quad (1)$$

$$(C_2H_5OH)_nH^+ + B \rightarrow BH^+ + nC_2H_5OH. \quad (2)$$

Here, "$B$" refers to amines and "$n$" is the number of reagent ions measured by the CIMS ($n = 1$–3). The $(C_2H_5OH)_2H^+$ ($m/z = 93$) peak was the highest among the three reagent ions ($m/z = 47$, 93, and 140). As shown in Fig. S2, the production ions of amines were protonated ions: $C_1$-amine ($m/z = 32$), $C_2$ ($m/z = 46$), $C_3$ ($m/z = 60$), $C_4$ ($m/z = 74$), $C_5$ ($m/z = 88$), and $C_6$ ($m/z = 102$). Ammonia product ions were $NH_4^+$ ($m/z = 18$, higher peak) and $(C_2H_5OH)NH_4^+$ ($m/z = 64$, lower peak); these two ions were strongly correlated to each other during the ammonia calibration and ambient measurements, indicating they represent ammonia signals.

To obtain a background signal, the CIMS is operated with 10 min of sampling followed by 10 min of background measurements. Figure S2 shows the main reagent and base compound product ions during the switching between ambient

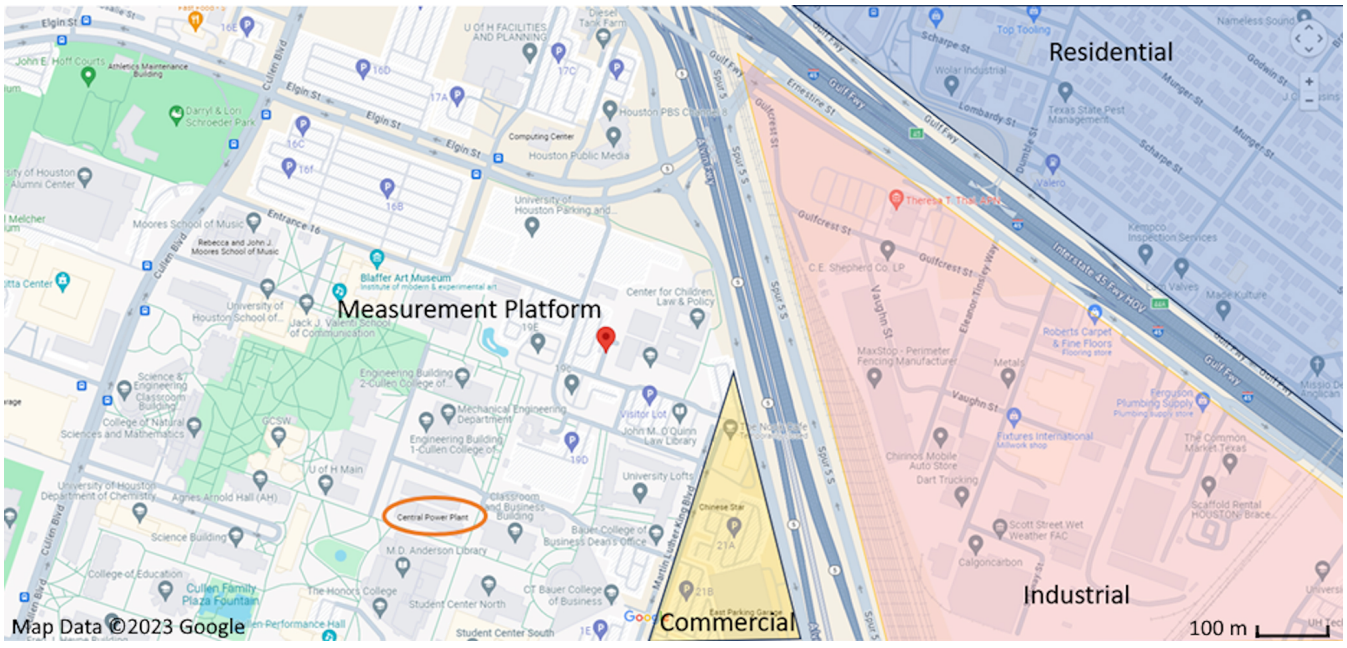


**Figure 1.** The location of the measurement platform is indicated by the red pin in the center of the map. Nearby commercial, industrial, and residential areas are labeled using yellow, red, and blue shading, respectively. The nearby University of Houston power plant is circled in orange to the southwest of the measurement platform. A map of the Greater Houston urban area and a satellite view of the nearby vicinity of the measurement site are shown in Fig. S1.

and background measurements. Background measurements were taken by switching a three-way valve to supply the inlet with a flow of zero air through a silicon phosphate medium (Pan Tech, Texas) to scrub ammonia and amines. The reagent signal was taken as the sum of three ethanol reagent ions. Reagent ion signals were typically around 400 kHz, with less than 10 % difference between the ambient and background measurement modes. Ammonia and amine concentrations were calculated by the difference between the ambient and background signals normalized to 1 000 000 Hz of reagent ion signal multiplied by a calibration factor. Calibration of the instrument was carried out with diluted ammonia in nitrogen and permeation tubes of methylamine, dimethylamine, trimethylamine, diethylamine, and diisopropylamine (Kintek, USA). Due to the difficulty of obtaining a calibration standard, $C_5$ amines were assumed to have the same sensitivity as $C_6$ amines. The calibration factors for each compound and detection limits were found to be similar to the results from the calibration of the instrument by You et al. (2014) (Table S1) over a period of nearly 10 years, demonstrating an excellent reproducibility in the instrument performance. The time response of the CIMS instrument to ammonia and amines is defined as where the signal stabilizes at its "double e-folded" concentration of $1/e^2$ during the calibration. Average response times for ammonia and amines were smaller than 1 min. For each 10 min cycle of background and measurement, the first 2 min of each background or measurement cycle were excluded from the data analysis to allow the instrument to reach a steady concentration.

The uncertainty in the CIMS included error in the permeation sources, which ranged from 2 % to 5 % depending on the compound. The permeation sources were diluted in two stages using flow controllers that each had uncertainties of 1.5 %. Total error in the calibration of the CIMS was 6.7 %. Overall uncertainty in the CIMS was 30 %, accounting for calibration error, variability of ion signals, and inlet losses.

Meteorological data were measured concurrently on the platform by a Vaisala HMP-45c for temperature and relative humidity and a RM Young 05305 wind speed and direction sensor. Additionally, CO and $NO_x$ ($NO + NO_2$) were measured with Thermo 48c and Thermo 42c-TL instruments, respectively. These measurements were provided by the University of Houston. The uncertainty in trace gas (CO and $NO_x$) measurements arises from instrumental uncertainty in the Thermo 48c CO analyzer and Thermo 42c-TL $NO_x$ analyzer. Zero correction was performed on this instrument daily by switching to a flow of zero air. The typical uncertainty of each of these instruments was 5 %.

## 3 Results and discussion

The time series of ammonia and amines during the ambient measurement period is shown in Fig. 2. The average ammonia concentration during the measurement campaign was 4 ppbv, with several short-term spikes above 10 ppbv and

one occasion when the concentration exceeded 20 ppbv. Concentrations of $C_1$ amine averaged 4 pptv with several spikes up to 15 pptv. Average $C_2$ amine concentrations were 6 pptv with frequent but brief periods of concentrations more than 10 pptv. Average $C_3$ amine concentrations were 31 pptv, with brief increases in concentration above 100 pptv. $C_4$ amine was the most abundant amine observed during the measurement period, with an average concentration of 79 pptv and spikes in concentration into the hundreds of pptv. Average $C_5$ and $C_6$ amine concentrations were 33 and 12 pptv, respectively. These concentrations in Houston were generally consistent with concentrations measured in other urban sites (Table 1). Previous CIMS ammonia measurements from aircraft flights above Houston observed similar baseline concentrations of ammonia (0.2–3 ppbv) with brief spikes in concentration (up to 80 ppbv) associated with agricultural or industrial activity (Nowak et al., 2010). Additionally, ammonia concentrations of similar magnitude to the high spikes in concentration observed in this study have been reported in Shanghai (Xiao et al., 2015) and at an urban site in Romania (Petrus et al., 2022), with high ammonia concentrations corresponding to high temperatures and high traffic activity. Long-term measurements taken in Nanjing with a cavity ring-down spectrometer also showed an average ammonia concentration of 12 ppbv (Liu et al., 2024). Measurements of amines in Atlanta, Georgia, showed $< 1$ to 3 pptv concentrations of $C_1$ and $C_2$ amines and $C_3$ and $C_6$ amines up to 15–25 pptv (Hanson et al., 2011). Yao et al. (2016) measured amines at the level of pptv or sub-pptv, e.g., $C_2$ amines of $3.9 \pm 1.2$ pptv, in urban Shanghai during the summer. It is possible that measured concentrations of amines measured here contain some interference from amides formed from oxidation of emitted amines. The CIMS does not have sufficient resolving power to separate trimethylamine ($m/z$ 59.11) from acetamide ($m/z$ 59.07). Therefore, these amine concentrations represent an upper limit of amine concentrations (assuming all of the detected signal is due to the presence of amines). However, Yao et al. (2016) measured amide concentrations in urban Shanghai of tens to hundreds of pptv, while $C_1$–$C_2$ amine concentrations in Shanghai were similar to the Houston observations reported here. Considering the consistency between amine measurements at these two urban locations, it is likely that interference from amides in the CIMS was minimal for $C_1$ and $C_2$ amines. The discrepancies between these two urban areas become more pronounced for $C_3$–$C_6$ amines (Table 1), which makes amide interference a possible explanation for elevated concentrations of $C_3$ amines and above.

Figure 3 shows the averaged diurnal concentrations of ammonia and amines during the observation period. Ammonia and amines had a diurnal cycle with peak concentrations in the afternoon with higher ambient temperatures. Generally, ammonia and amines correlated with one another throughout the measurement campaign, while $C_1$–$C_3$ amines showed the highest correlation with ammonia. Peak concentrations of all compounds corresponded with the high temperature of the day at around 15:00 LT (local time). This was especially pronounced for ammonia and $C_1$ and $C_3$ amines. The relationships between ammonia and amines and temperature are shown in Fig. 4. Ammonia concentrations (ppbv) had the strongest correlation with temperature (K), and the relationship fit an exponential parameterization, as shown in the following equation:

$$[NH_3] = 2.85 + 9.66 \times 10^{15}\, e^{-\frac{10619}{T}}. \quad (3)$$

Amines generally showed linear relationships with temperature, with $C_3$ and $C_4$ amines displaying the strongest relationships. $C_3$ amines increased by 2.3 pptv $K^{-1}$ ($r^2 = 0.86$), and $C_4$ increased by 2.9 pptv $K^{-1}$ ($r^2 = 0.65$). $C_5$ and $C_6$ amines were also moderately correlated with temperature, increasing by 1.2 and 0.5 pptv $K^{-1}$, respectively ($r^2 = 0.60$ for both $C_5$ and $C_6$). On the other hand, the correlations of $C_1$ and $C_2$ amines with temperature were weaker: $C_1$ only increased by 0.1 pptv $K^{-1}$ with almost no correlation ($r^2 = 0.22$), and $C_2$ increased by 0.8 pptv $K^{-1}$ ($r^2 = 0.50$). The temperature dependence of ammonia and amines was previously observed in a rural forest in Alabama by You et al. (2014), who attributed this partially to particle-to-gas conversion of ammonia- and amine-containing particles at elevated temperatures. The temperature dependence could also be due to higher emissions at higher temperatures. The temperature dependence of ammonia and amines has been observed at other urban, suburban, and rural locations such as Kent, Ohio (You et al., 2014), Atlanta (Hanson et al., 2011), Delaware (Freshour et al., 2014), the southern Great Plains (Freshour et al., 2014), and in rural central Germany (Kürten et al., 2016).

Anthropogenic pollutants such as CO and $NO_x$ and CO can serve as tracers for industrial and traffic activities. Ammonia and amines in general showed a positive correlation with CO, with the exception of $C_3$ amines (Fig. 5). As ammonia, amines, and CO can be traced to traffic or industrial emissions, the positive relationship between these compounds implies that these base compounds were emitted from pollutant sources. Unlike with CO, there was a negative correlation with $NO_x$ (Fig. S3). This lack of a strong correlation between $NO_x$ and ammonia was previously observed in Nanjing, where a strong reduction in $NO_x$ concentration during COVID-19 lockdown periods was not accompanied by an equivalent reduction in ammonia concentrations (Liu et al., 2024). This may indicate some unique emission sources for ammonia and amines that do not co-emit $NO_x$.

Wind speed and direction can help to identify local sources of ammonia and amines near the measurement site. Figures 6 and S4 show the correlation of ammonia and amines with wind speeds and direction throughout the observation period. Consistent between all base compounds is the high concentration coming from the southeast. This is the direction of the interstate highway, industrial areas, and train yards (Figs. 1

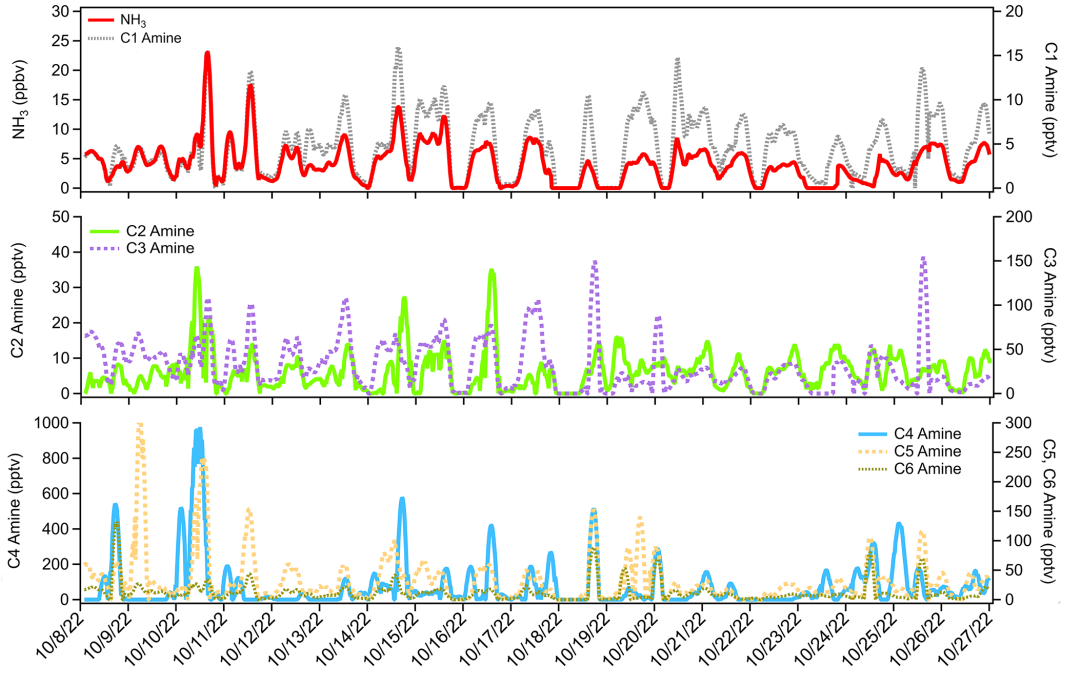


**Figure 2.** Time series of ammonia and $C_1$–$C_6$ amines observed at the urban center in Houston, Texas, in October 2022.

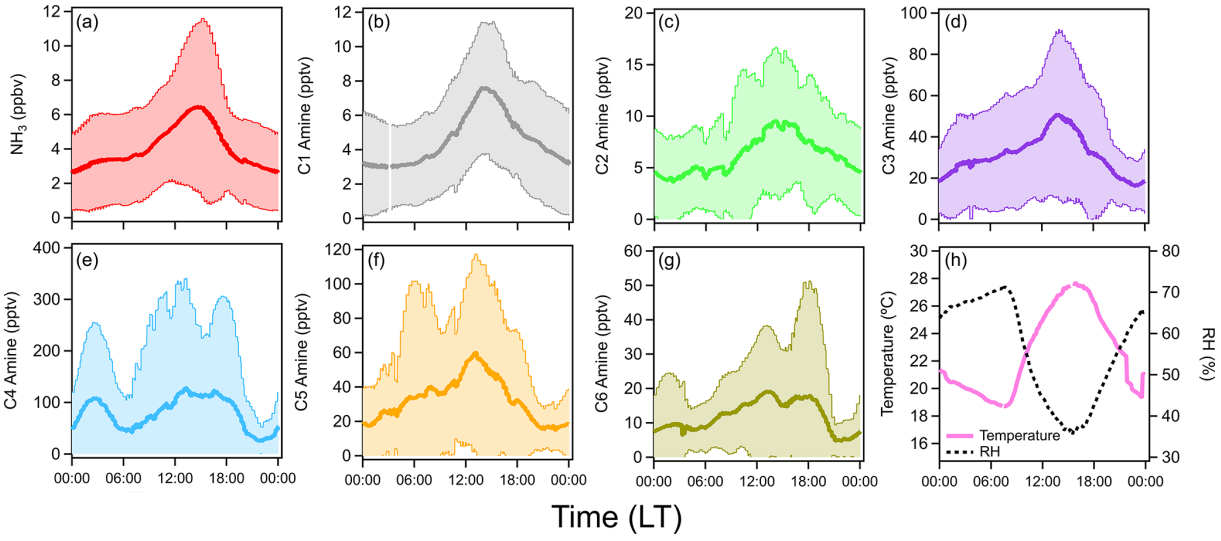


**Figure 3.** Averaged diurnal cycles of **(a)** ammonia, **(b–g)** $C_1$–$C_6$ amines, and **(h)** temperature and RH in Houston, Texas, during the observation period (19 d continuously). Shaded areas indicate a standard deviation from the mean values of observation data.

and S1). Ammonia and most amines also have a pronounced source from the northwest – this is the direction of downtown Houston, where population density is highest. Except for $C_2$ and $C_4$ amines, the observed ammonia and amines in Houston were higher during periods of low wind speeds. The abundant $C_2$ and $C_4$ at high wind speeds may suggest that $C_2$ and $C_4$ amines were transported from more distant sources.

Figure S5 shows the average diurnal cycle of ammonia and amines on weekdays as opposed to weekends. With the exception of $C_2$ and $C_4$ amines, there was a clear decrease in concentrations during weekends during the afternoon peak. Weekends saw much less traffic and activity on the University of Houston campus. During this observation period, ambient temperatures were higher during the weekends, which would increase emissions. Therefore, the differences in weekdays vs. weekends indicate that amines and ammonia were indeed emitted from traffic and industrial activities. Lower average amine concentrations on weekends

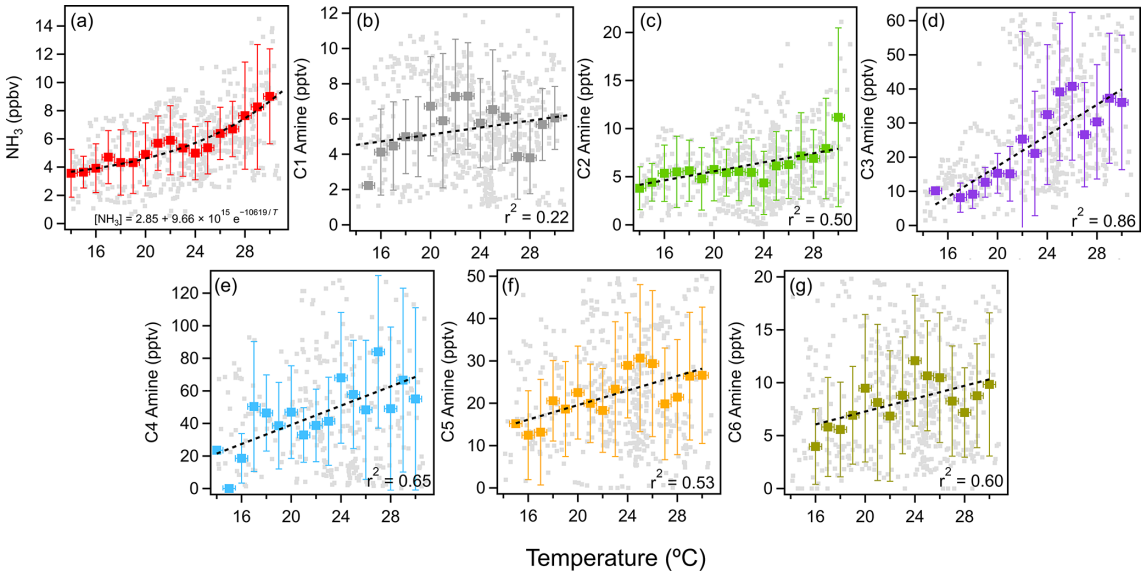


**Figure 4.** Temperature dependence of **(a)** ammonia and **(b–g)** $C_1$–$C_6$ amines measured in Houston. Vertical bars indicate a standard deviation from the mean values of observation data. Binned temperatures are shown as colored squares, 1 min averaged data are shown as gray squares. Horizontal bars indicate bin width. Dashed black lines indicate the exponential fit for ammonia and linear fits for amines.

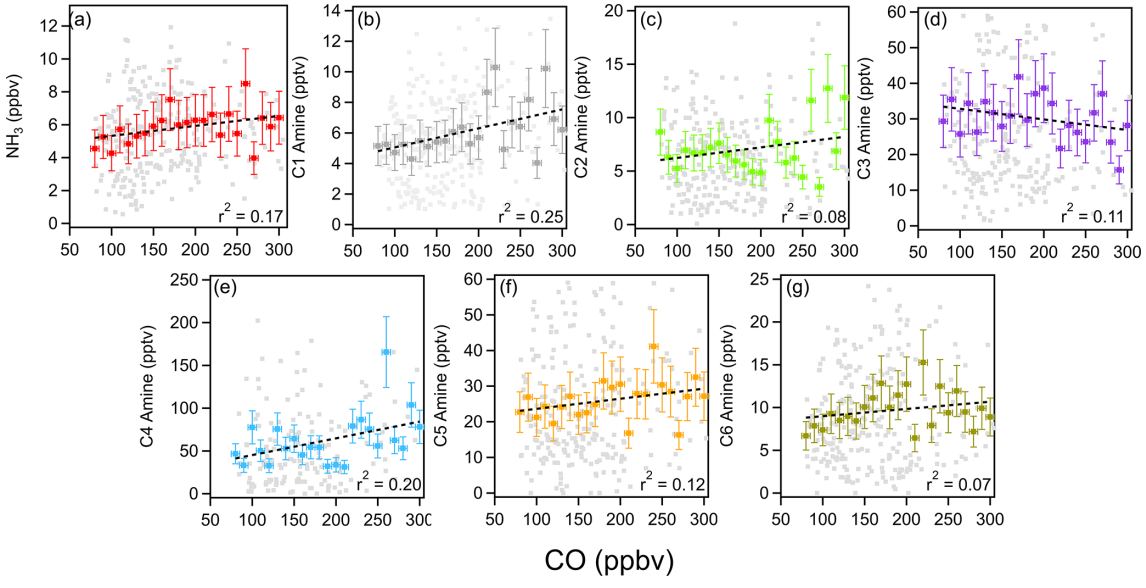


**Figure 5.** Correlation between ammonia **(a)** and $C_1$–$C_6$ amines **(b–g)** with the colocated CO concentrations during the measurement campaign. Binned CO concentrations are shown as colored squares, 5 min averaged data are shown as gray squares. Vertical bars indicate a standard deviation from the mean values of observation data. Horizontal bars indicate bin widths. Dashed black lines indicate linear fits.

were also observed during mobile measurements in Yangtze River Delta cities (Chang et al., 2022).

## 4 Atmospheric implications

Field observations show that sulfuric acid and amines are responsible for aerosol nucleation (Yao et al., 2016; Yan et al., 2021; Cai et al., 2021; Cai et al., 2023; Jen et al., 2016; Smith et al., 2010; Brean et al., 2020); however, currently global models do not have amine emission inventories. Figure 7 shows the correlation of ammonia with $C_1$–$C_6$ amines measured during this campaign. This figure also includes that data obtained with the same instrument in Kent, Ohio (You et al., 2014). It is clear from this figure that concentrations of ammonia and $C_1$, $C_2$, $C_3$, $C_5$, and $C_6$ amines were positively correlated with one another throughout the study: $r^2$

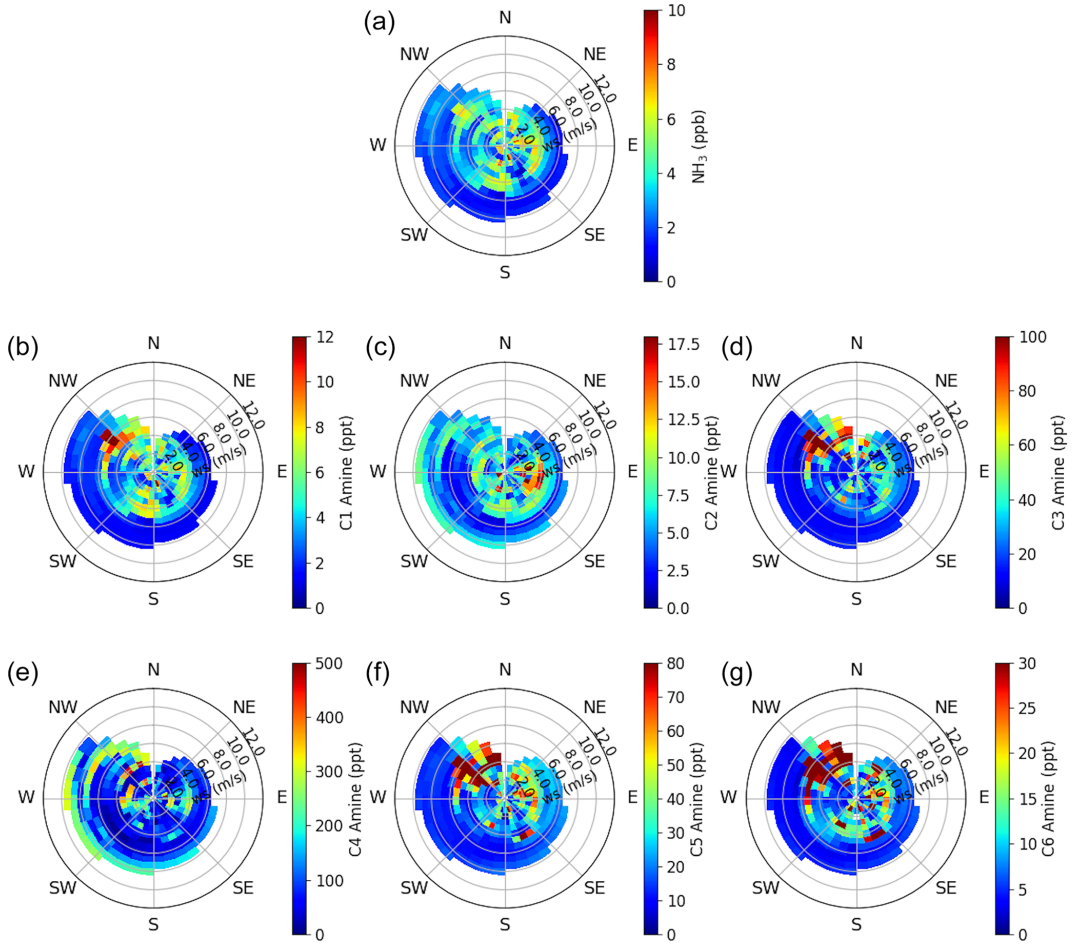


**Figure 6.** Wind rose plots of **(a)** ammonia and **(b-g)** $C_1$–$C_6$ amines observed in urban Houston. The color scale indicates concentration, and the radial intensity shows the wind speed.

values for the correlation between ammonia and amines were 0.61 for $C_1$, 0.42 for $C_2$, 0.47 for $C_3$, 0.26 for $C_5$, and 0.88 for $C_6$. These relationships imply that these compounds are mostly co-emitted from similar sources and undergo similar atmospheric transport. $C_4$ amines showed no correlation with ammonia and lower-mass amines – the $r^2$ value for $C_4$ vs. $NH_3$ was 0.048. This indicates a unique source for $C_4$ amines, consistent with both elevated $C_4$ concentrations at high wind speeds and higher weekend $C_4$ concentrations as discussed previously. Correlations of $C_1$–$C_3$ amines concentrations, taken from the linear fits of the plots shown in Fig. 7, were approximately equivalent to $1.1 \times 10^{-3}$ [$NH_3$], $1.4 \times 10^{-3}$ [$NH_3$], and $8.4 \times 10^{-3}$ [$NH_3$], respectively. $C_5$ and $C_6$ amine concentrations were $1.9 \times 10^{-2}$ [$NH_3$] and $3.5 \times 10^{-3}$ [$NH_3$], respectively (Table S2). From these results, we propose that global modelers use 0.1 % of the ammonia concentration as a proxy of dimethylamine to simulate urban NPF processes. However, this recommendation comes with the caveat that measured $C_2$ amines may include dimethylamine and ethylamine due to the inability of mass spectrometry to resolve isomers. Therefore, this correlation represents only the upper bound of dimethylamine concentrations.

From these observations made in very polluted Houston and less polluted Kent, we propose that dimethylamine concentrations can be estimated using the proxy of 0.1 % ammonia concentrations at the polluted sites in the United States. The caveat of this proxy is that it is based on only two locations in the United States and did not consider different emission sectors. There has so far been only one attempt to use quantify the aerosol nucleation processes using sulfuric acid and dimethylamine in the global model, performed by Zhao et al. (2024), and they concluded that this nucleation process is dominant globally in the polluted boundary layer in China, India, Europe, and the United States. In this cited study the authors used the proxy of dimethylamine using ammonia concentrations; for example, they used dimethylamine/ammonia ratios of 0.0070, 0.0018, and 0.0100, for chemical industrial, other industrial, and residential sources, respectively; these proxies were derived by Mao et al. (2018) based

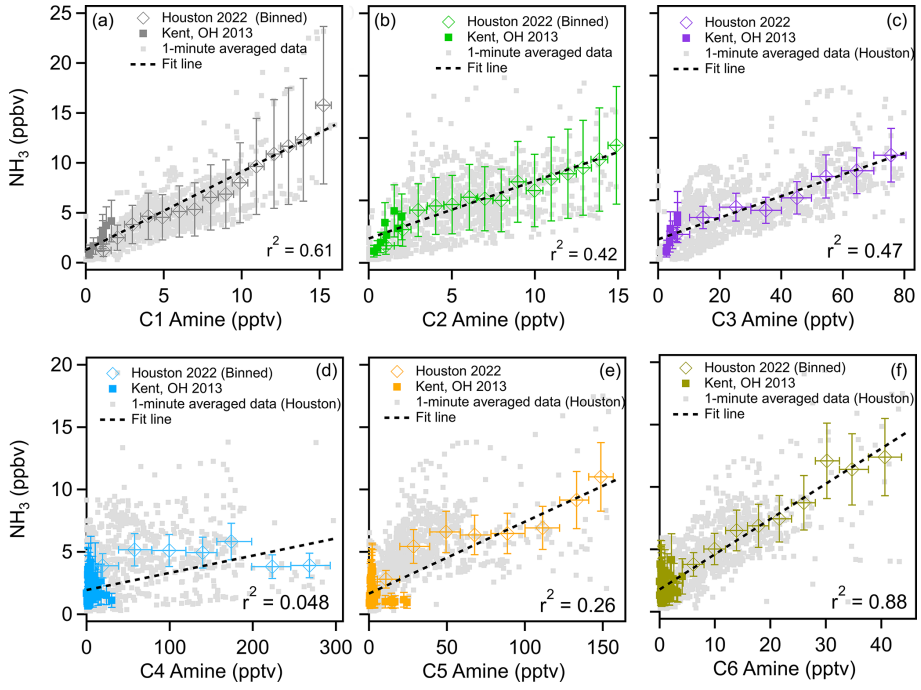


**Figure 7.** Correlations of $C_1$–$C_6$ amines with ammonia throughout the observation period in Houston, TX (diamonds), and Kent, OH (squares), as reported by You et al. (2014). Binned concentrations are shown as colored squares, 1 min averaged data from Houston are shown as gray squares. Vertical bars indicate a standard deviation from the mean values of observation data. Horizontal bars indicate bin widths. Dashed black lines indicate linear fits of the combined data from Kent and Houston.

on measurements made in Nanjing (Zheng et al., 2015). Our observations indicate that Zhao et al. (2024) likely overestimated dimethylamine concentrations for polluted sites in the United States overall and thus overpredicted nucleation rates as well. Thus, our results can provide a more constrained proxy for polluted sites in the United States for future modeling studies.

## 5 Conclusions

Our observations in urban Houston show that ammonia and amines generally followed a clear diurnal cycle, peaking in the early afternoon when the ambient temperature was highest during the day. We found a correlation between ammonia or amines and ambient temperature. The diurnal cycles and temperature dependence of these compounds are consistent with (You et al., 2014) which showed that the gas-to-particle conversion contributes to the temperature dependence. To verify this process, the chemical composition of particle is needed, but particle measurements were not available during the present study. Additionally, the observed temperature dependence could be due to increased emissions of ammonia and amines from biogenic and anthropogenic sources. On the other hand, photochemical aging that occurs typically during the higher solar flux can also reduce the gas phase amines at the noontime; thus, photochemical aging was unlikely the main driving factor to produce higher concentrations of amines around noon.

High concentrations of ammonia and amines were correlated with local air masses from densely populated areas and areas of high traffic, industry, and other human activity. This suggests that most ammonia and amines measured in Houston originated from pollutant sources, consistent with the correlation observed with CO concentrations. There was also a clear increase in ammonia and amines on days with more human activity, as shown by the results of concentrations on weekends vs. weekdays. We observed a consistent relationship between ammonia and amines during our measurement campaign and with observations in the less densely populated area of Kent, Ohio, suggesting that it is reasonable to parameterize amine emission inventories based on existing ammonia inventories to simulate urban NPF processes. However, as the CIMS is incapable of resolving amides or isomers, this parameterization is only capable of representing the upper bounds of amines. Further work involving instrumentation capable of isomer resolution such as tandem MS/MS or chromatographic separation is needed to determine typical isomer ratios of amines for more accurate parameterizations.

Measuring ammonia and amines in the atmosphere is one of the most challenging areas in the development of atmospheric analytical instruments (Lee, 2022; Lee et al., 2019). The CIMS used in this campaign is currently one of the few

instruments in the world that is capable of simultaneous measurements of ammonia and amines at atmospherically relevant detection limits and timescales. Very importantly, our CIMS, despite its relatively low mass resolution, has measured ammonia and amines at various atmospheric conditions, including rural forests (You et al., 2014; Kanawade et al., 2014), a relatively less polluted site (Yu and Lee, 2012; You et al., 2014; Erupe et al., 2010), and an extremely polluted urban environment (this study), with consistent instrument sensitivities over the decade; to our knowledge, this is the only instrument that demonstrated such consistency in the performance. Studies have shown that the co-presence of ammonia and amines can enhance sulfuric acid nucleation rates compared to ammonia alone (Yu et al., 2012; Glasoe et al., 2015; Myllys et al., 2019). From this perspective, simultaneous measurements of ammonia and amines will be required for the correct prediction of NPF processes in the atmosphere. Measurements of ammonia and amines with comprehensive calibration as shown in the present study are even rarer, but such measurements are needed for mitigating urban air quality problems and the health effects of ultrafine particles.

**Code and data availability.** The data used in this study are available from the Zenodo repository site (https://doi.org/10.5281/zenodo.11086677, Tiszenkel et al., 2024). The code used in this study will be available upon request from the corresponding author (shanhu.lee@uah.edu).

**Supplement.** The supplement related to this article is available online at: https://doi.org/10.5194/acp-24-11351-2024-supplement.

**Author contributions.** SHL designed the research. LT and SHL performed measurements. JHF provided the measurement platform and the trace gas and meteorology data. LT and SHL wrote the manuscript.

**Competing interests.** The contact author has declared that none of the authors has any competing interests.

**Disclaimer.** Publisher's note: Copernicus Publications remains neutral with regard to jurisdictional claims made in the text, published maps, institutional affiliations, or any other geographical representation in this paper. While Copernicus Publications makes every effort to include appropriate place names, the final responsibility lies with the authors.

**Acknowledgements.** We acknowledge funding support from the National Science Foundation (grant nos. 2209722, 2117389, and 2107916) and the Texas Commission on Environmental Quality (grant no. 582-22-31535-018).

**Financial support.** This research has been supported by the National Science Foundation (grant nos. 2209722, 2117389, and 2107916) and the Texas Commission on Environmental Quality (grant no. 582-22-31535-018).

**Review statement.** This paper was edited by Theodora Nah and reviewed by two anonymous referees.

## References

Almeida, J., Schobesberger, S., Kürten, A., Ortega, I. K., Kupiainen-Määttä, O., Praplan, A. P., Adamov, A., Amorim, A., Bianchi, F., Breitenlechner, M., David, A., Dommen, J., Donahue, N. M., Downard, A., Dunne, E., Duplissy, J., Ehrhart, S., Flagan, R. C., Franchin, A., Guida, R., Hakala, J., Hansel, A., Heinritzi, M., Henschel, H., Jokinen, T., Junninen, H., Kajos, M., Kangasluoma, J., Keskinen, H., Kupc, A., Kurtén, T., Kvashin, A. N., Laaksonen, A., Lehtipalo, K., Leiminger, M., Leppä, J., Loukonen, V., Makhmutov, V., Mathot, S., McGrath, M. J., Nieminen, T., Olenius, T., Onnela, A., Petäjä, T., Riccobono, F., Riipinen, I., Rissanen, M., Rondo, L., Ruuskanen, T., Santos, F. D., Sarnela, N., Schallhart, S., Schnitzhofer, R., Seinfeld, J. H., Simon, M., Sipilä, M., Stozhkov, Y., Stratmann, F., Tomé, A., Tröstl, J., Tsagkogeorgas, G., Vaattovaara, P., Viisanen, Y., Virtanen, A., Vrtala, A., Wagner, P. E., Weingartner, E., Wex, H., Williamson, C., Wimmer, D., Ye, P., Yli-Juuti, T., Carslaw, K. S., Kulmala, M., Curtius, J., Baltensperger, U., Worsnop, D. R., Vehkamäki, H., and Kirkby, J.: Molecular understanding of sulphuric acid–amine particle nucleation in the atmosphere, Nature, 502, 359–363, https://doi.org/10.1038/nature12663, 2013.

Beck, L. J., Sarnela, N., Junninen, H., Hoppe, C. J. M., Garmash, O., Bianchi, F., Riva, M., Rose, C., Peräkylä, O., Wimmer, D., Kausiala, O., Jokinen, T., Ahonen, L., Mikkilä, J., Hakala, J., He, X.-C., Kontkanen, J., Wolf, K. K. E., Cappelletti, D., Mazzola, M., Traversi, R., Petroselli, C., Viola, A. P., Vitale, V., Lange, R., Massling, A., Nøjgaard, J. K., Krejci, R., Karlsson, L., Zieger, P., Jang, S., Lee, K., Vakkari, V., Lampilahti, J., Thakur, R. C., Leino, K., Kangasluoma, J., Duplissy, E.-M., Siivola, E., Marbouti, M., Tham, Y. J., Saiz-Lopez, A., Petäjä, T., Ehn, M., Worsnop, D. R., Skov, H., Kulmala, M., Kerminen, V.-M., and Sipilä, M.: Differing Mechanisms of New Particle Formation at Two Arctic Sites, Geophys. Res. Lett., 48, e2020GL091334, https://doi.org/10.1029/2020GL091334, 2021.

Benson, D. R., Markovich, A., Al-Refai, M., and Lee, S. H.: A Chemical Ionization Mass Spectrometer for ambient measurements of Ammonia, Atmos. Meas. Tech., 3, 1075–1087, https://doi.org/10.5194/amt-3-1075-2010, 2010.

Bianchi, F., Tröstl, J., Junninen, H., Frege, C., Henne, S., Hoyle, C. R., Molteni, U., Herrmann, E., Adamov, A., Bukowiecki, N., Chen, X., Duplissy, J., Gysel, M., Hutterli, M., Kangasluoma, J., Kontkanen, J., Kürten, A., Manninen, H. E., Münch, S., Peräkylä, O., Petäjä, T., Rondo, L., Williamson, C., Weingartner, E., Curtius, J., Worsnop, D. R., Kulmala, M., Dommen, J., and Bal-

tensperger, U.: New particle formation in the free troposphere: A question of chemistry and timing, Science, 352, 1109–1112, https://doi.org/10.1126/science.aad5456, 2016.

Brean, J., Beddows, D. C. S., Shi, Z., Temime-Roussel, B., Marchand, N., Querol, X., Alastuey, A., Minguillón, M. C., and Harrison, R. M.: Molecular insights into new particle formation in Barcelona, Spain, Atmos. Chem. Phys., 20, 10029–10045, https://doi.org/10.5194/acp-20-10029-2020, 2020.

Brean, J., Dall'Osto, M., Simó, R., Shi, Z., Beddows, D. C. S., and Harrison, R. M.: Open ocean and coastal new particle formation from sulfuric acid and amines around the Antarctic Peninsula, Nat. Geosci., 14, 383–388, https://doi.org/10.1038/s41561-021-00751-y, 2021.

Cai, R., Yan, C., Yang, D., Yin, R., Lu, Y., Deng, C., Fu, Y., Ruan, J., Li, X., Kontkanen, J., Zhang, Q., Kangasluoma, J., Ma, Y., Hao, J., Worsnop, D. R., Bianchi, F., Paasonen, P., Kerminen, V. M., Liu, Y., Wang, L., Zheng, J., Kulmala, M., and Jiang, J.: Sulfuric acid–amine nucleation in urban Beijing, Atmos. Chem. Phys., 21, 2457–2468, https://doi.org/10.5194/acp-21-2457-2021, 2021.

Cai, R., Yin, R., Li, X., Xie, H.-B., Yang, D., Kerminen, V.-M., Smith, J. N., Ma, Y., Hao, J., Chen, J., Kulmala, M., Zheng, J., Jiang, J., and Elm, J.: Significant contributions of trimethylamine to sulfuric acid nucleation in polluted environments, npj Clim. Atmos. Sci., 6, 75, https://doi.org/10.1038/s41612-023-00405-3, 2023.

Chang, Y., Wang, H., Gao, Y., Jing, S. a., Lu, Y., Lou, S., Kuang, Y., Cheng, K., Ling, Q., Zhu, L., Tan, W., and Huang, R.-J.: Nonagricultural Emissions Dominate Urban Atmospheric Amines as Revealed by Mobile Measurements, Geophys. Res. Lett., 49, e2021GL097640, https://doi.org/10.1029/2021GL097640, 2022.

Ellis, R. A., Murphy, J. G., Pattey, E., van Haarlem, R., O'Brien, J. M., and Herndon, S. C.: Characterizing a Quantum Cascade Tunable Infrared Laser Differential Absorption Spectrometer (QC-TILDAS) for measurements of atmospheric ammonia, Atmos. Meas. Tech., 3, 397–406, https://doi.org/10.5194/amt-3-397-2010, 2010.

Erupe, M. E., Benson, D. R., Li, J., Young, L.-H., Verheggen, B., Al-Refai, M., Tahboub, O., Cunningham, V., Frimpong, F., Viggiano, A. A., and Lee, S.-H.: Correlation of aerosol nucleation rate with sulfuric acid and ammonia in Kent, Ohio: An atmospheric observation, J. Geophys. Res.-Atmos., 115, D23216, https://doi.org/10.1029/2010JD013942, 2010.

Erupe, M. E., Viggiano, A. A., and Lee, S.-H.: The effect of trimethylamine on atmospheric nucleation involving H2SO4, Atmos. Chem. Phys., 11, 4767–4775, https://doi.org/10.5194/acp-11-4767-2011, 2011.

Freshour, N. A., Carlson, K. K., Melka, Y. A., Hinz, S., Panta, B., and Hanson, D. R.: Amine permeation sources characterized with acid neutralization and sensitivities of an amine mass spectrometer, Atmos. Meas. Tech., 7, 3611–3621, https://doi.org/10.5194/amt-7-3611-2014, 2014.

Ge, X., Wexler, A. S., and Clegg, S. L.: Atmospheric amines – Part I. A review, Atmos. Environ., 45, 524–546, https://doi.org/10.1016/j.atmosenv.2010.10.012, 2011a.

Ge, X., Wexler, A. S., and Clegg, S. L.: Atmospheric amines – Part II. Thermodynamic properties and gas/-particle partitioning, Atmos. Environ., 45, 561–577, https://doi.org/10.1016/j.atmosenv.2010.10.013, 2011b.

Glasoe, W. A., Volz, K., Panta, B., Freshour, N., Bachman, R., Hanson, D. R., McMurry, P. H., and Jen, C.: Sulfuric acid nucleation: an experimental study of the effect of seven bases, J. Geophys. Res., 120, 1933–1950, https://doi.org/10.1002/2014JD022730, 2015.

Griffith, D. W. T. and Galle, B.: Flux measurements of $NH_3$, $N_2O$ and $CO_2$ using dual beam FTIR spectroscopy and the flux–gradient technique, Atmos. Environ., 34, 1087–1098, https://doi.org/10.1016/S1352-2310(99)00368-4, 2000.

Gu, B., Zhang, L., Van Dingenen, R., Vieno, M., Van Grinsven, H. J. M., Zhang, X., Zhang, S., Chen, Y., Wang, S., Ren, C., Rao, S., Holland, M., Winiwarter, W., Chen, D., Xu, J., and Sutton, M. A.: Abating ammonia is more cost-effective than nitrogen oxides for mitigating $PM_{2.5}$ air pollution, Science, 374, 758–762, https://doi.org/10.1126/science.abf8623, 2021.

Hanson, D. R., McMurry, P. H., Jiang, J., Tanner, D., and Huey, L. G.: Ambient Pressure Proton Transfer Mass Spectrometry: Detection of Amines and Ammonia, Environ. Sci. Technol., 45, 8881–8888, https://doi.org/10.1021/es201819a, 2011.

Jen, C. N., Bachman, R., Zhao, J., McMurry, P. H., and Hanson, D. R.: Diamine-sulfuric acid reactions are a potent source of new particle formation, Geophys. Res. Lett., 43, 867–873, https://doi.org/10.1002/2015GL066958, 2016.

Jokinen, T., Sipilä, M., Kontkanen, J., Vakkari, V., Tisler, P., Duplissy, E. M., Junninen, H., Kangasluoma, J., Manninen, H. E., Petäjä, T., Kulmala, M., Worsnop, D. R., Kirkby, J., Virkkula, A., and Kerminen, V. M.: Ion-induced sulfuric acid–ammonia nucleation drives particle formation in coastal Antarctica, Sci. Adv., 4, eaat9744, https://doi.org/10.1126/sciadv.aat9744, 2018.

Kanawade, V. P., Tripathi, S. N., Siingh, D., Gautam, A. S., Srivastava, A. K., Kamra, A. K., Soni, V. K., and Sethi, V.: Observations of new particle formation at two distinct Indian subcontinental urban locations, Atmos. Environ., 96, 370–379, https://doi.org/10.1016/j.atmosenv.2014.08.001, 2014.

Köllner, F., Schneider, J., Willis, M. D., Klimach, T., Helleis, F., Bozem, H., Kunkel, D., Hoor, P., Burkart, J., Leaitch, W. R., Aliabadi, A. A., Abbatt, J. P. D., Herber, A. B., and Borrmann, S.: Particulate trimethylamine in the summertime Canadian high Arctic lower troposphere, Atmos. Chem. Phys., 17, 13747–13766, https://doi.org/10.5194/acp-17-13747-2017, 2017.

Kürten, A., Bergen, A., Heinritzi, M., Leiminger, M., Lorenz, V., Piel, F., Simon, M., Sitals, R., Wagner, A. C., and Curtius, J.: Observation of new particle formation and measurement of sulfuric acid, ammonia, amines and highly oxidized organic molecules at a rural site in central Germany, Atmos. Chem. Phys., 16, 12793–12813, https://doi.org/10.5194/acp-16-12793-2016, 2016.

Lee, S.-H.: Perspective on the Recent Measurements of Reduced Nitrogen Compounds in the Atmosphere, Front. Environ. Sci., 10, 868534, https://doi.org/10.3389/fenvs.2022.868534, 2022.

Lee, S.-H., Gordon, H., Yu, H., Lehtipalo, K., Haley, R., Li, Y., and Zhang, R.: New Particle Formation in the Atmosphere: From Molecular Clusters to Global Climate, J. Geophys. Res.-Atmos., 124, 7098–7146, https://doi.org/10.1029/2018JD029356, 2019.

Leen, J. B., Yu, X.-Y., Gupta, M., Baer, D. S., Hubbe, J. M., Kluzek, C. D., Tomlinson, J. M., and Hubbell II, M. R.: Fast In Situ Airborne Measurement of Ammonia Using a Mid-Infrared Off-Axis ICOS Spectrometer, Environ. Sci. Technol., 47, 10446–10453, https://doi.org/10.1021/es401134u, 2013.

Lehtipalo, K., Yan, C., Dada, L., Bianchi, F., Xiao, M., Wagner, R., Stolzenburg, D., Ahonen, L. R., Amorim, A., Baccarini, A., Bauer, P. S., Baumgartner, B., Bergen, A., Bernhammer, A.-K., Breitenlechner, M., Brilke, S., Buchholz, A., Mazon, S. B., Chen, D., Chen, X., Dias, A., Dommen, J., Draper, D. C., Duplissy, J., Ehn, M., Finkenzeller, H., Fischer, L., Frege, C., Fuchs, C., Garmash, O., Gordon, H., Hakala, J., He, X., Heikkinen, L., Heinritzi, M., Helm, J. C., Hofbauer, V., Hoyle, C. R., Jokinen, T., Kangasluoma, J., Kerminen, V.-M., Kim, C., Kirkby, J., Kontkanen, J., Kürten, A., Lawler, M. J., Mai, H., Mathot, S., Mauldin, R. L., Molteni, U., Nichman, L., Nie, W., Nieminen, T., Ojdanic, A., Onnela, A., Passananti, M., Petäjä, T., Piel, F., Pospisilova, V., Quéléver, L. L. J., Rissanen, M. P., Rose, C., Sarnela, N., Schallhart, S., Schuchmann, S., Sengupta, K., Simon, M., Sipilä, M., Tauber, C., Tomé, A., Tröstl, J., Väisänen, O., Vogel, A. L., Volkamer, R., Wagner, A. C., Wang, M., Weitz, L., Wimmer, D., Ye, P., Ylisirniö, A., Zha, Q., Carslaw, K. S., Curtius, J., Donahue, N. M., Flagan, R. C., Hansel, A., Riipinen, I., Virtanen, A., Winkler, P. M., Baltensperger, U., Kulmala, M., and Worsnop, D. R.: Multicomponent new particle formation from sulfuric acid, ammonia, and biogenic vapors, Sci. Adv., 4, eaau5363, https://doi.org/10.1126/sciadv.aau5363, 2018.

Liu, R., Liu, T., Huang, X., Ren, C., Wang, L., Niu, G., Yu, C., Zhang, Y., Wang, J., Qi, X., Nie, W., Chi, X., and Ding, A.: Characteristics and sources of atmospheric ammonia at the SORPES station in the western Yangtze river delta of China, Atmos. Environ., 318, 120234, https://doi.org/10.1016/j.atmosenv.2023.120234, 2024.

Malloy, Q. G. J., Li, Q., Warren, B., Cocker Iii, D. R., Erupe, M. E., and Silva, P. J.: Secondary organic aerosol formation from primary aliphatic amines with $NO_3$ radical, Atmos. Chem. Phys., 9, 2051–2060, https://doi.org/10.5194/acp-9-2051-2009, 2009.

Mao, J., Yu, F., Zhang, Y., An, J., Wang, L., Zheng, J., Yao, L., Luo, G., Ma, W., Yu, Q., Huang, C., Li, L., and Chen, L.: High-resolution modeling of gaseous methylamines over a polluted region in China: source-dependent emissions and implications of spatial variations, Atmos. Chem. Phys., 18, 7933–7950, https://doi.org/10.5194/acp-18-7933-2018, 2018.

Martin, N. A., Ferracci, V., Cassidy, N., and Hoffnagle, J. A.: The application of a cavity ring-down spectrometer to measurements of ambient ammonia using traceable primary standard gas mixtures, Appl. Phys. B, 122, 219, https://doi.org/10.1007/s00340-016-6486-9, 2016.

McManus, J. B., Mark, S. Z., David, D. N., Jr., Joanne, H. S., Scott, C. H., Ezra, C. W., and Rick, W.: Application of quantum cascade lasers to high-precision atmospheric trace gas measurements, Opt. Eng., 49, 111124, https://doi.org/10.1117/1.3498782, 2010.

Miller, D. J., Sun, K., Tao, L., Khan, M. A., and Zondlo, M. A.: Open-path, quantum cascade-laser-based sensor for high-resolution atmospheric ammonia measurements, Atmos. Meas. Tech., 7, 81–93, https://doi.org/10.5194/amt-7-81-2014, 2014.

Myllys, N., Chee, S., Olenius, T., Lawler, M., and Smith, J.: Molecular-Level Understanding of Synergistic Effects in Sulfuric Acid–Amine–Ammonia Mixed Clusters, J. Phys. Chem. A, 123, 2420–2425, https://doi.org/10.1021/acs.jpca.9b00909, 2019.

Nielsen, C. J.: Atmospheric Degradation of Amines (ADA), Summary report: Photo-oxidation of methylamine, dimethylamine and trimethylamine, CLIMIT project no. 201604, Norge, Norsk Institutt for Luftforskning, ISBN 978-82-425-2357-0, 2016.

Nielsen, C. J., Herrmann, H., and Weller, C.: Atmospheric chemistry and environmental impact of the use of amines in carbon capture and storage (CCS), Chem. Soc. Rev., 41, 6684–6704, https://doi.org/10.1039/C2CS35059A, 2012.

Nowak, J. B., Huey, L. G., Russell, A. G., Tian, D., Neuman, J. A., Orsini, D., Sjostedt, S. J., Sullivan, A. P., Tanner, D. J., Weber, R. J., Nenes, A., Edgerton, E., and Fehsenfeld, F. C.: Analysis of urban gas phase ammonia measurements from the 2002 Atlanta Aerosol Nucleation and Real-Time Characterization Experiment (ANARChE), J. Geophys. Res.-Atmos., 111, D17308, https://doi.org/10.1029/2006JD007113, 2006.

Nowak, J. B., Neuman, J. A., Bahreini, R., Brock, C. A., Middlebrook, A. M., Wollny, A. G., Holloway, J. S., Peischl, J., Ryerson, T. B., and Fehsenfeld, F. C.: Airborne observations of ammonia and ammonium nitrate formation over Houston, Texas, J. Geophys. Res.-Atmos., 115, D22304, https://doi.org/10.1029/2010JD014195, 2010.

Petrus, M., Popa, C., and Bratu, A. M.: Ammonia Concentration in Ambient Air in a Peri-Urban Area Using a Laser Photoacoustic Spectroscopy Detector, Materials, 15, 3182, https://doi.org/10.3390/ma15093182, 2022.

Pollack, I. B., Lindaas, J., Roscioli, J. R., Agnese, M., Permar, W., Hu, L., and Fischer, E. V.: Evaluation of ambient ammonia measurements from a research aircraft using a closed-path QC-TILDAS operated with active continuous passivation, Atmos. Meas. Tech., 12, 3717–3742, https://doi.org/10.5194/amt-12-3717-2019, 2019.

Pushkarsky, M. B., Webber, M. E., Baghdassarian, O., Narasimhan, L. R., and Patel, C. K. N.: Laser-based photoacoustic ammonia sensors for industrial applications, Appl. Phys. B, 75, 391–396, https://doi.org/10.1007/s00340-002-0967-8, 2002.

Qiu, C. and Zhang, R.: Multiphase chemistry of atmospheric amines, Phys. Chem. Chem. Phys., 15, 5738–5752, https://doi.org/10.1039/C3CP43446J, 2013.

Schwab, J. J., Li, Y., Bae, M. S., Demerjian, K. L., Hou, J., Zhou, X., Jensen, B., and Pryor, S. C.: A laboratory intercomparison of real-time gaseous ammonia measurement methods, Environ. Sci. Technol., 41, 8412–8419, https://doi.org/10.1021/es070354r, 2007.

Silva, P. J., Erupe, M. E., Price, D., Elias, J., Malloy, G. J. Q., Li, Q., Warren, B., and Cocker, D. R., III: Trimethylamine as Precursor to Secondary Organic Aerosol Formation via Nitrate Radical Reaction in the Atmosphere, Environ. Sci. Technol., 42, 4689–4696, https://doi.org/10.1021/es703016v, 2008.

Smith, J. N., Barsanti, K. C., Friedli, H. R., Ehn, M., Kulmala, M., Collins, D. R., Scheckman, J. H., Williams, B. J., and McMurry, P. H.: Observations of aminium salts in atmospheric nanoparticles and possible climatic implications, P. Natl. Acad. Sci. USA, 107, 6634–6639, 2010.

Tiszenkel, L., Flynn, J., and Lee, S.: Data Used in Manuscript Entitled "Measurement Report: Urban Ammonia and Amines in Houston, Texas", Zenodo [data set], https://doi.org/10.5281/zenodo.13685879, 2024.

Wang, G., Zhang, R., Gomez, M. E., Yang, L., Levy Zamora, M., Hu, M., Lin, Y., Peng, J., Guo, S., Meng, J., Li, J., Cheng, C., Hu, T., Ren, Y., Wang, Y., Gao, J., Cao, J., An, Z., Zhou, W., Li, G., Wang, J., Tian, P., Marrero-Ortiz, W., Secrest, J., Du, Z.,

Zheng, J., Shang, D., Zeng, L., Shao, M., Wang, W., Huang, Y., Wang, Y., Zhu, Y., Li, Y., Hu, J., Pan, B., Cai, L., Cheng, Y., Ji, Y., Zhang, F., Rosenfeld, D., Liss, P. S., Duce, R. A., Kolb, C. E., and Molina, M. J.: Persistent sulfate formation from London Fog to Chinese haze, P. Natl. Acad. Sci. USA, 113, 13630–13635, https://doi.org/10.1073/pnas.1616540113, 2016.

Wang, M., Kong, W., Marten, R., He, X.-C., Chen, D., Pfeifer, J., Heitto, A., Kontkanen, J., Dada, L., Kürten, A., Yli-Juuti, T., Manninen, H. E., Amanatidis, S., Amorim, A., Baalbaki, R., Baccarini, A., Bell, D. M., Bertozzi, B., Bräkling, S., Brilke, S., Murillo, L. C., Chiu, R., Chu, B., De Menezes, L.-P., Duplissy, J., Finkenzeller, H., Carracedo, L. G., Granzin, M., Guida, R., Hansel, A., Hofbauer, V., Krechmer, J., Lehtipalo, K., Lamkaddam, H., Lampimäki, M., Lee, C. P., Makhmutov, V., Marie, G., Mathot, S., Mauldin, R. L., Mentler, B., Müller, T., Onnela, A., Partoll, E., Petäjä, T., Philippov, M., Pospisilova, V., Ranjithkumar, A., Rissanen, M., Rörup, B., Scholz, W., Shen, J., Simon, M., Sipilä, M., Steiner, G., Stolzenburg, D., Tham, Y. J., Tomé, A., Wagner, A. C., Wang, D. S., Wang, Y., Weber, S. K., Winkler, P. M., Wlasits, P. J., Wu, Y., Xiao, M., Ye, Q., Zauner-Wieczorek, M., Zhou, X., Volkamer, R., Riipinen, I., Dommen, J., Curtius, J., Baltensperger, U., Kulmala, M., Worsnop, D. R., Kirkby, J., Seinfeld, J. H., El-Haddad, I., Flagan, R. C., and Donahue, N. M.: Rapid growth of new atmospheric particles by nitric acid and ammonia condensation, Nature, 581, 184–189, https://doi.org/10.1038/s41586-020-2270-4, 2020.

Wang, Y., Yang, G., Lu, Y., Liu, Y., Chen, J., and Wang, L.: Detection of gaseous dimethylamine using vocus proton-transfer-reaction time-of-flight mass spectrometry, Atmos. Environ., 243, 117875, https://doi.org/10.1016/j.atmosenv.2020.117875, 2020.

Xiao, M., Hoyle, C. R., Dada, L., Stolzenburg, D., Kürten, A., Wang, M., Lamkaddam, H., Garmash, O., Mentler, B., Molteni, U., Baccarini, A., Simon, M., He, X. C., Lehtipalo, K., Ahonen, L. R., Baalbaki, R., Bauer, P. S., Beck, L., Bell, D., Bianchi, F., Brilke, S., Chen, D., Chiu, R., Dias, A., Duplissy, J., Finkenzeller, H., Gordon, H., Hofbauer, V., Kim, C., Koenig, T. K., Lampilahti, J., Lee, C. P., Li, Z., Mai, H., Makhmutov, V., Manninen, H. E., Marten, R., Mathot, S., Mauldin, R. L., Nie, W., Onnela, A., Partoll, E., Petäjä, T., Pfeifer, J., Pospisilova, V., Quéléver, L. L. J., Rissanen, M., Schobesberger, S., Schuchmann, S., Stozhkov, Y., Tauber, C., Tham, Y. J., Tomé, A., Vazquez-Pufleau, M., Wagner, A. C., Wagner, R., Wang, Y., Weitz, L., Wimmer, D., Wu, Y., Yan, C., Ye, P., Ye, Q., Zha, Q., Zhou, X., Amorim, A., Carslaw, K., Curtius, J., Hansel, A., Volkamer, R., Winkler, P. M., Flagan, R. C., Kulmala, M., Worsnop, D. R., Kirkby, J., Donahue, N. M., Baltensperger, U., El Haddad, I., and Dommen, J.: The driving factors of new particle formation and growth in the polluted boundary layer, Atmos. Chem. Phys., 21, 14275–14291, https://doi.org/10.5194/acp-21-14275-2021, 2021.

Xiao, S., Wang, M. Y., Yao, L., Kulmala, M., Zhou, B., Yang, X., Chen, J. M., Wang, D. F., Fu, Q. Y., Worsnop, D. R., and Wang, L.: Strong atmospheric new particle formation in winter in urban Shanghai, China, Atmos. Chem. Phys., 15, 1769–1781, https://doi.org/10.5194/acp-15-1769-2015, 2015.

Yan, C., Yin, R., Lu, Y., Dada, L., Yang, D., Fu, Y., Kontkanen, J., Deng, C., Garmash, O., Ruan, J., Baalbaki, R., Schervish, M., Cai, R., Bloss, M., Chan, T., Chen, T., Chen, Q., Chen, X., Chen, Y., Chu, B., Dällenbach, K., Foreback, B., He, X., Heikkinen, L., Jokinen, T., Junninen, H., Kangasluoma, J., Kokkonen, T., Kurppa, M., Lehtipalo, K., Li, H., Li, H., Li, X., Liu, Y., Ma, Q., Paasonen, P., Rantala, P., Pileci, R. E., Rusanen, A., Sarnela, N., Simonen, P., Wang, S., Wang, W., Wang, Y., Xue, M., Yang, G., Yao, L., Zhou, Y., Kujansuu, J., Petäjä, T., Nie, W., Ma, Y., Ge, M., He, H., Donahue, N. M., Worsnop, D. R., Veli-Matti, K., Wang, L., Liu, Y., Zheng, J., Kulmala, M., Jiang, J., and Bianchi, F.: The Synergistic Role of Sulfuric Acid, Bases, and Oxidized Organics Governing New-Particle Formation in Beijing, Geophys. Res. Lett., 48, e2020GL091944, https://doi.org/10.1029/2020GL091944, 2021.

Yao, L., Wang, M. Y., Wang, X. K., Liu, Y. J., Chen, H. F., Zheng, J., Nie, W., Ding, A. J., Geng, F. H., Wang, D. F., Chen, J. M., Worsnop, D. R., and Wang, L.: Detection of atmospheric gaseous amines and amides by a high-resolution time-of-flight chemical ionization mass spectrometer with protonated ethanol reagent ions, Atmos. Chem. Phys., 16, 14527–14543, https://doi.org/10.5194/acp-16-14527-2016, 2016.

You, Y., Kanawade, V. P., de Gouw, J. A., Guenther, A. B., Madronich, S., Sierra-Hernández, M. R., Lawler, M., Smith, J. N., Takahama, S., Ruggeri, G., Koss, A., Olson, K., Baumann, K., Weber, R. J., Nenes, A., Guo, H., Edgerton, E. S., Porcelli, L., Brune, W. H., Goldstein, A. H., and Lee, S.-H.: Atmospheric amines and ammonia measured with a chemical ionization mass spectrometer (CIMS), Atmos. Chem. Phys., 14, 12181–12194, https://doi.org/10.5194/acp-14-12181-2014, 2014.

Yu, H. and Lee, S. H.: A chemical ionization mass spectrometer for the detection of atmospheric amines, Environ. Chem., 9, 190–201, 2012

Yu, H., McGraw, R., and Lee, S. H.: Effects of amines on formation of sub-3 nm particles and their subsequent growth, Geophys. Res. Lett., 39, L02807, https://doi.org/10.1029/2011gl050099, 2012.

Zhao, B., Donahue, N. M., Zhang, K., Mao, L., Shrivastava, M., Ma, P.-L., Shen, J., Wang, S., Sun, J., Gordon, H., Tang, S., Fast, J., Wang, M., Gao, Y., Yan, C., Singh, B., Li, Z., Huang, L., Lou, S., Lin, G., Wang, H., Jiang, J., Ding, A., Nie, W., Qi, X., Chi, X., and Wang, L.: Global variability in atmospheric new particle formation mechanisms, Nature, 631, 98–105, https://doi.org/10.1038/s41586-024-07547-1, 2024.

Zheng, J., Ma, Y., Chen, M., Zhang, Q., Wang, L., Khalizov, A. F., Yao, L., Wang, Z., Wang, X., and Chen, L.: Measurement of atmospheric amines and ammonia using the high resolution time-of-flight chemical ionization mass spectrometry, Atmos. Environ., 102, 249–259, https://doi.org/10.1016/j.atmosenv.2014.12.002, 2015.

Zhu, S., Yan, C., Zheng, J., Chen, C., Ning, H., Yang, D., Wang, M., Ma, Y., Zhan, J., Hua, C., Yin, R., Li, Y., Liu, Y., Jiang, J., Yao, L., Wang, L., Kulmala, M., and Worsnop, D. R.: Observation and Source Apportionment of Atmospheric Alkaline Gases in Urban Beijing, Environ. Sci. Technol., 56, 17545–17555, https://doi.org/10.1021/acs.est.2c03584, 2022.